

Some Design Considerations for a Large Solid Angle Charged Plus Neutrals
Detector for e^+e^- Storage Rings

Terry Mast and Jerry Nelson

Lawrence Berkeley Laboratory
University of California
Berkeley, California 94720

August 1974

ABSTRACT

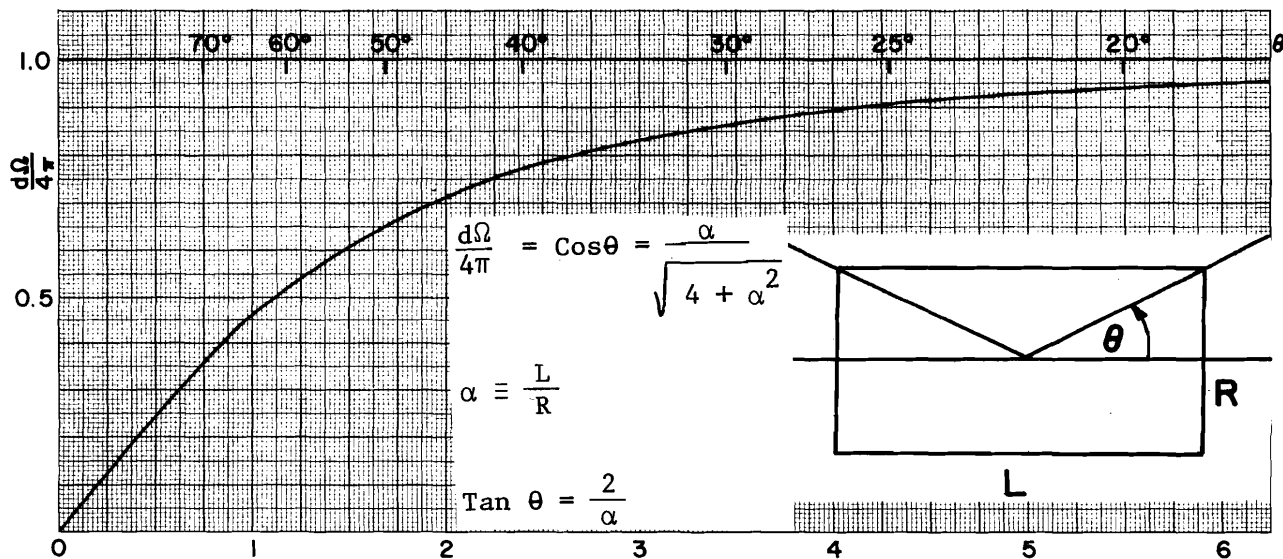
We describe here the relations between various design parameters, costs, resolutions, geometry, etc., that we have found useful in thinking about charged and neutral particle detectors for SPEAR and PEP. A great many alternatives exist for the various components of these detectors: solenoid vs. Helmholtz coils for the magnet, normal versus superconducting magnets, active convertors versus passive convertors for the gammas, different gamma detection methods, different return yoke configurations, etc. We have thought most about a system based upon a solenoid magnet with drift chambers inside for charged particle detection and lead glass outside for gamma detection. Consequently most of the formulae and figures in this paper are oriented toward that configuration. A great many other configurations have been discussed as possibilities for PEP detectors. Since the constraints (\$, manpower, electrical power) and the physics of interest at PEP are still unknown we consider the present configuration to be only one of many possibilities. Each of the possible configurations needs to be carefully studied to understand its limitations and to optimize the design within those limitations. In that spirit we present here some of the tools needed for understanding the design of a solenoidal detector.

We consider various aspects of the detector in the following sections.

- | | |
|------------------------------------|------|
| 1. Solid Angle | P 2 |
| 2. Solenoid Thickness | P 3 |
| 3. Magnet Design | P 4 |
| 4. Charged Particle Resolution | P 9 |
| 5. Charged Particle Discrimination | P 11 |
| 6. Neutrals Resolution | P 21 |
| 7. Cost of Neutrals Detector | P 26 |

1. SOLID ANGLE

The low event rate and the difficulties of understanding many particle final states have convinced most of us that we need a large solid angle detector. To define some notation and get a feel for solid angles we calculate the solid angle subtended by a cylinder of length L and radius R. The aspect ratio α is L/R. The solid angle is plotted as a function of α in Fig. 1.



XBL 7410-1961

Fig. 1.

2. Solenoid Thickness

Gamma converting in the magnet coil will suffer an unknown energy loss. Thus the coil should have a small number of radiation lengths to convert as few gammas as possible and should have a small dE/dx to reduce the loss from those gammas which do convert. The optimum material is Aluminum. It has low resistivity (3.5×10^{-8} ohm-meter), a long radiation length (9.0 cm), a low dE/dx (4.3 MeV/cm), is inexpensive, and is easily worked. Although copper has a factor of 1.6 less resistivity, its radiation length is only 1.45 cm and its dE/dx is 12.9 MeV/cm. The fraction of gammas converting in a thickness x is given by $1 - e^{-x/X(E)}$, where $X(E)$ is the conversion length for a gamma of energy E . Fig. 2 shows the number of gammas converting versus thickness of aluminum for various energy gammas.

The fraction of gammas converting in a thickness x is given by $1 - e^{-x/X(E)}$, where $X(E)$ is the conversion length for a gamma of energy E .

The energy loss in the coil for gammas that do convert can be easily calculated for a small coil thickness ($\leq X_0$) by assuming that one pair is formed. The ionization loss of the pair if it begins at the beginning of the coil will be $2(x)(dE/dx)$. Assuming the pairs originate uniformly throughout the thickness we get a mean energy loss of $(x)(dE/dx)$ and the rms spread is $2(x)(dE/dx)/\sqrt{12}$. The fractional rms energy loss for various energy converting gammas is plotted versus aluminum thickness in Fig. 3. Also shown are curves for the resolution of lead glass and NaI. For example, if we are interested in measuring 100 MeV gammas with lead glass the coil thickness should be less than 0.7 radiation lengths in order not to seriously degrade the resolution of the lead glass. If we are using the NaI the coil thickness should be less than 0.1 radiation lengths. We emphasize again that this degradation only takes place for the fraction that convert. In practice

one must take into account that gammas traverse the coil at a variety of angles and that cooling water (radiation length = 36 cm) must be added to the coil.

3. Magnet Design

Since the power available for the magnet is a strong constraint on any design we list here some related equations to give a feeling for the dependence on various parameters.

P = power (watts)

$\mu_0 = 4\pi \times 10^{-7}$ meter-tesla/amp

B = field at center of solenoid (tesla) (1 tesla = 10 kilogauss)

h = conductor thickness (m)

w = conductor width (m)

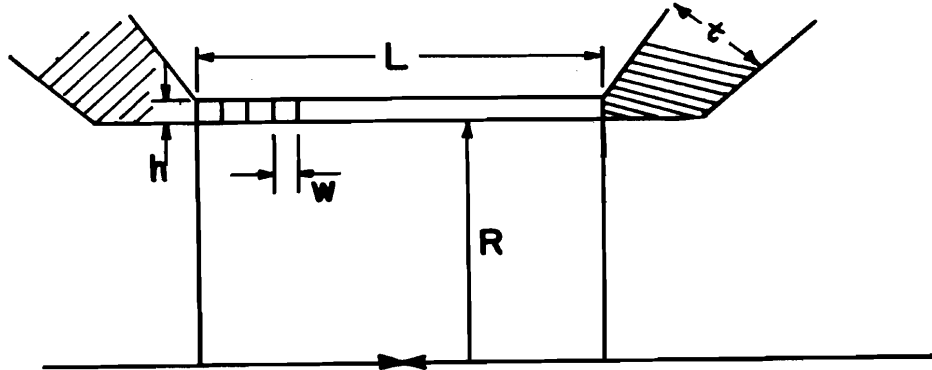
R = radius of solenoid (m)

L = length of solenoid (m)

n = turns/meter

I = current (amps)

ρ = resistivity (ohm-meter) $\rho(\text{Cu}) = 2.2 \times 10^{-8}$ (ohm-meter) at 85°C
 $\rho(\text{Al}) = 3.5 \times 10^{-8}$ (ohm-meter)

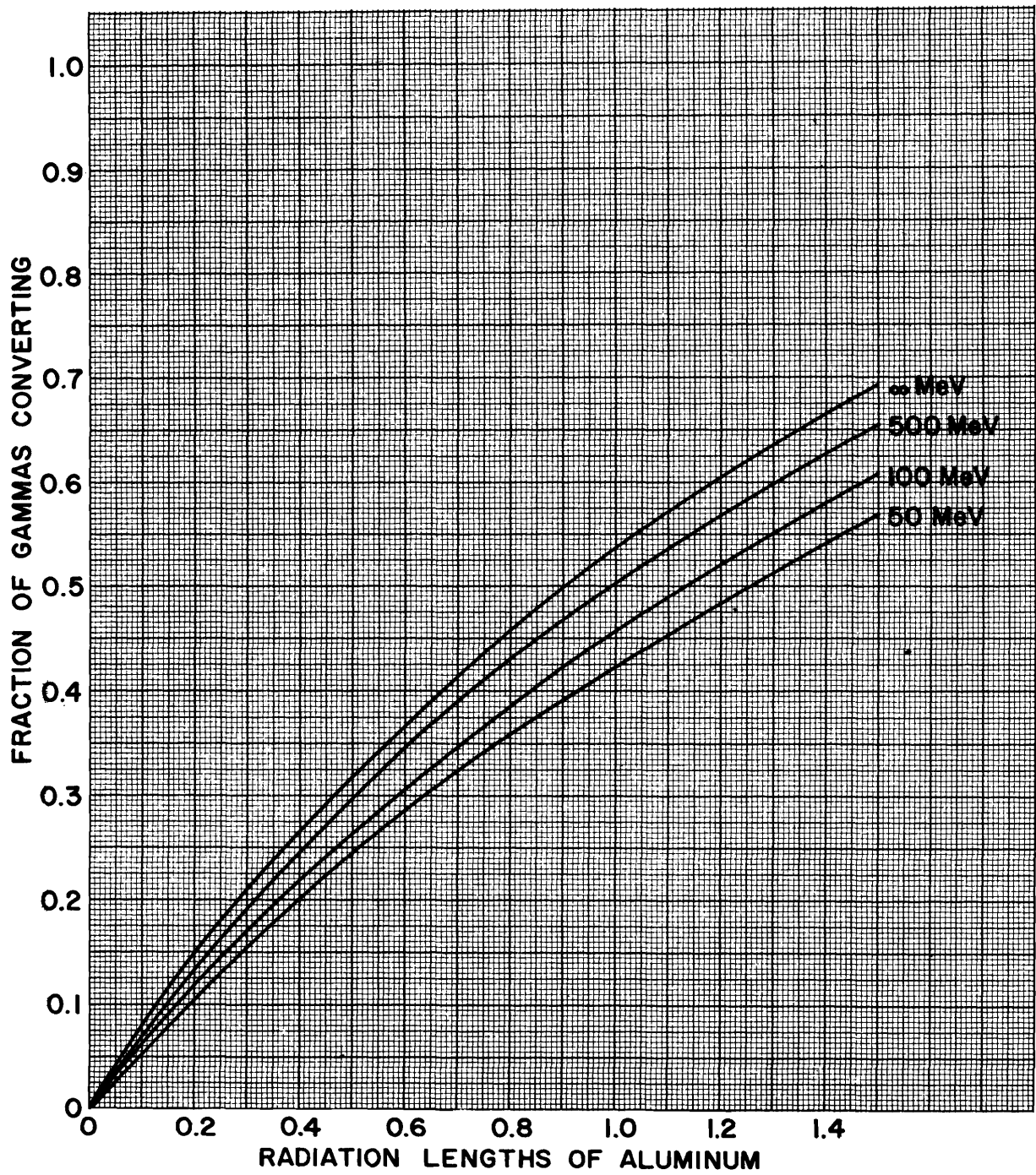


$$B = \mu_0 I n f$$

$$P = \frac{B^2 2\pi\rho L}{f^2 \mu_0^2 \ln(1 + h/R)}$$

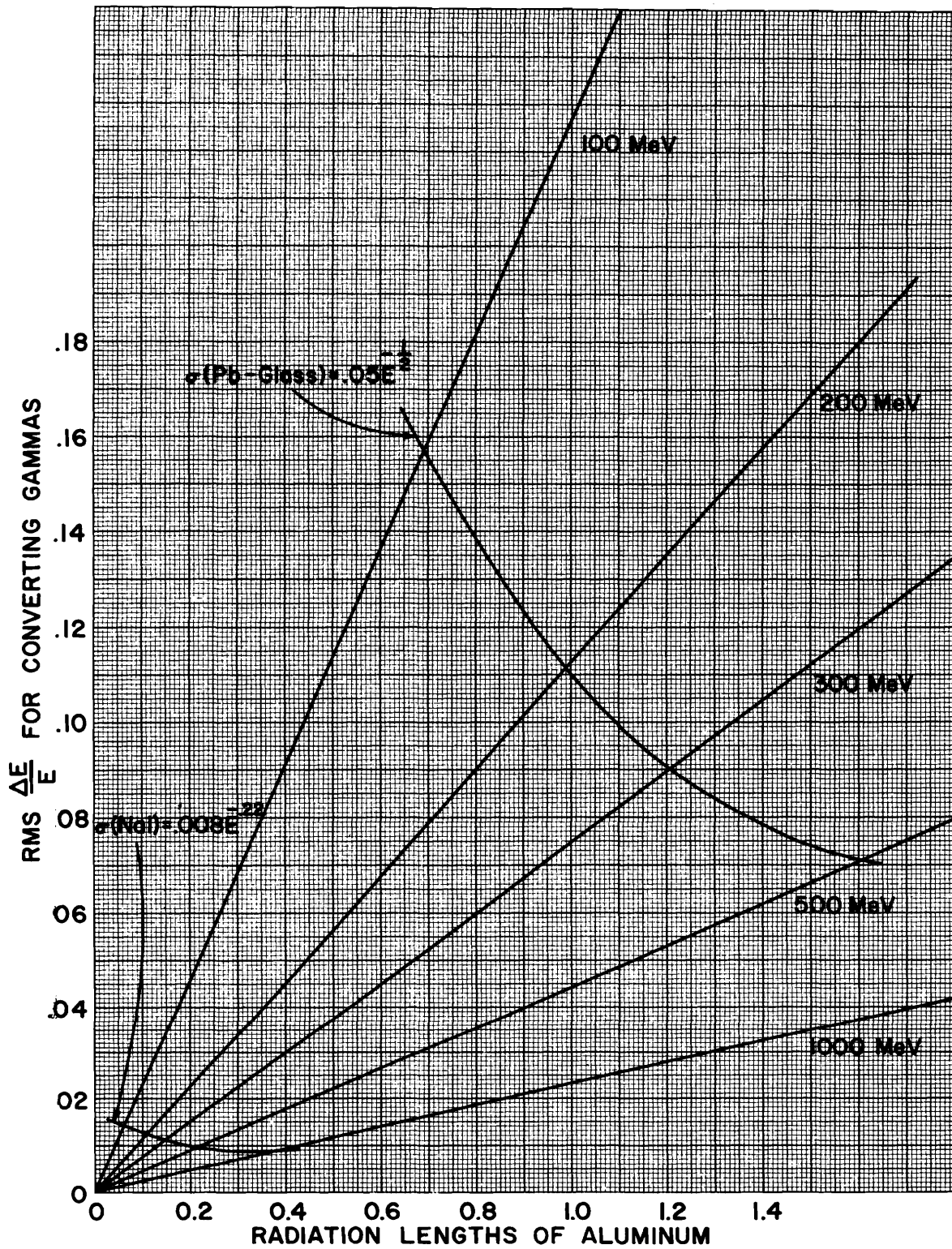
$$V \text{ (volts)} = \frac{B 2\pi\rho L}{\mu_0 f w \ln(1 + h/R)}$$

$$\text{current density (amps/m}^2\text{)} = \frac{B}{\mu_0 f h}$$



XBL 7410-1957

Fig. 2.



XBL 7410-1962

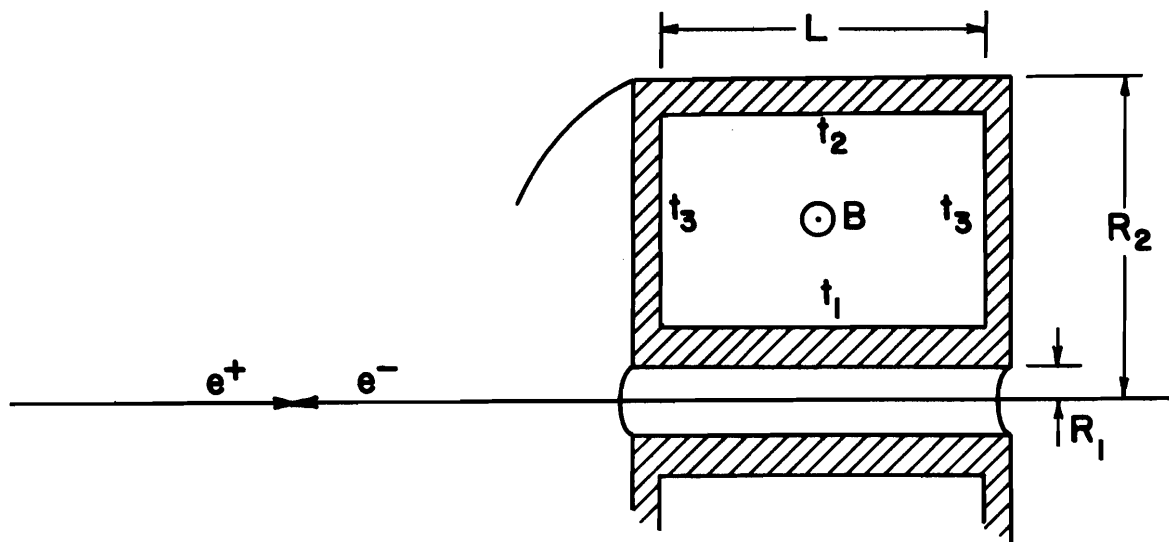
Fig. 3.

The factor f depends on how the solenoid ends are treated. For an infinitely long solenoid or one which has iron return yokes closing the ends $f = 1.0$. For a return yoke which does not close the ends (as shown) $f = 0.97$. For a solenoid without return yokes $f = (1 + (\frac{2R}{L})^2)^{-1/2}$.

For a field of 0.5 tesla in an aluminum coil 3 cm thick, 0.5 m radius, and 2.0 m long ($f=1.0$) we need 0.96 Megawatts and 1330 amps/cm².

If no end caps are required for the return yoke (the field remains uniform to $\pm 5\%$ in the central region) then the return yoke need only subtend a small solid angle. The thickness of the iron at the radius R is given by $t = \frac{BR}{2B_y}$, where B_y is the field in the iron (typically 1.4 to 1.6). The fraction of the solid angle subtended by such a return yoke is $(\cos \theta_1 - \cos \theta_2)$ where $\tan \theta_1 = 2R/L$ and $\tan \theta_2 = 2R/(L+2t)$. For a field of 0.5 tesla, $B_y = 1.5$, $L=2.0$ and $R = .5$ the return yoke thickness is 8.3 cm and it subtends 1.3% of 4π .

Since the momentum resolution is poor in the end region with a solenoidal field we could add to each end of the main detector end cap detectors consisting of toroidal magnets, drift chambers, and gamma detectors. We calculate here the power needed for a simple toroidal magnet. The length, radii, and conductor thicknesses are defined in the figure below.



Using the same units as on the previous page we have

$$B = \frac{\mu_0 I}{2 \pi r} \quad , \quad \text{Let } \bar{B} = \frac{\mu_0 I}{\pi (R_1 + R_2)} \text{ the field at } r = (R_1 + R_2)/2$$

$$P = \frac{2\pi (R_1 + R_2)^2 \bar{B}^2}{\mu_0^2} \left[\frac{\rho_3 \ln(R_2/R_1)}{t_3} + \frac{\rho_2 L}{2R_2 t_2 - t_2^2} + \frac{\rho_1 L}{2R_1 t_1 + t_1^2} \right]$$

The thickness t_3 should be chosen thin enough so as not to degrade the energy resolution of gammas. For example choose $t_3 = 1.5$ cm of aluminum and let $R_1 = 0.1$, $R_2 = 0.5$ and $L=1.0$. The inner and outer cylinders can be made of copper and we can choose $t_2 = 5$ cm, and $t_1 = 4$ cm. With a \bar{B} of .15 tesla each magnet will require 0.17 Megawatts.

4. Charged Particle Momentum Resolution

The uncertainty in the momentum measurement in the drift chambers comes from the uncertainty in the track positions in the chambers and the multiple coulomb scattering in the chambers.

Define Δx = position measurement uncertainty (m) (for drift chambers = .0001)

B = field (tesla)

p = momentum (GeV/c)

S = radial distance between first and last chamber (m)

x/X_0 = radiation lengths of material in chamber

θ = angle of the track from the beam

Assuming scattering measurement error in the central chamber alone the momentum resolution is

$$\frac{\Delta p}{p} = \frac{1}{SB} \left[\left(\frac{27 (\Delta x) p \sin \theta}{S} \right)^2 + \left(\frac{0.1}{\beta \sqrt{\sin \theta}} \sqrt{\frac{x}{X_0}} \right)^2 \right]^{1/2}$$

The first term comes from the measurement uncertainty and is proportional to the momentum and the second term comes from the multiple coulomb scattering and dominates at low momentum. We have assumed perfect knowledge of the angle θ . (If θ is measured by a measurement on z (to $\pm \delta z$) at a radius R , then $\delta z \cos \theta \sin \theta / R$ must be added in quadrature to the above $\delta p/p$. For a $\delta z = \pm 1$ cm this generally makes a negligible contribution to the error.) Figure 4 shows the resolution versus p for 45° and 90° . Curves are shown for $S = 25$ cm and $S = 75$ cm. These would correspond to magnets of .5 and 1.0 meters radius since room must be left for beam pipe and supports and framing for chambers. We've assumed a field of .5 tesla, $\Delta x = .0001$, and

.0066 radiation lengths of material. Also plotted is the contribution of the measurement error alone showing the importance of including the multiple coulomb scattering. Fig. 5 shows the variation with θ for 0.2 and 1.0 GeV/c.

The above formula is of course only an approximation to a complete treatment which must take into account the multiple measurements of the track and the scattering from the distributed material.

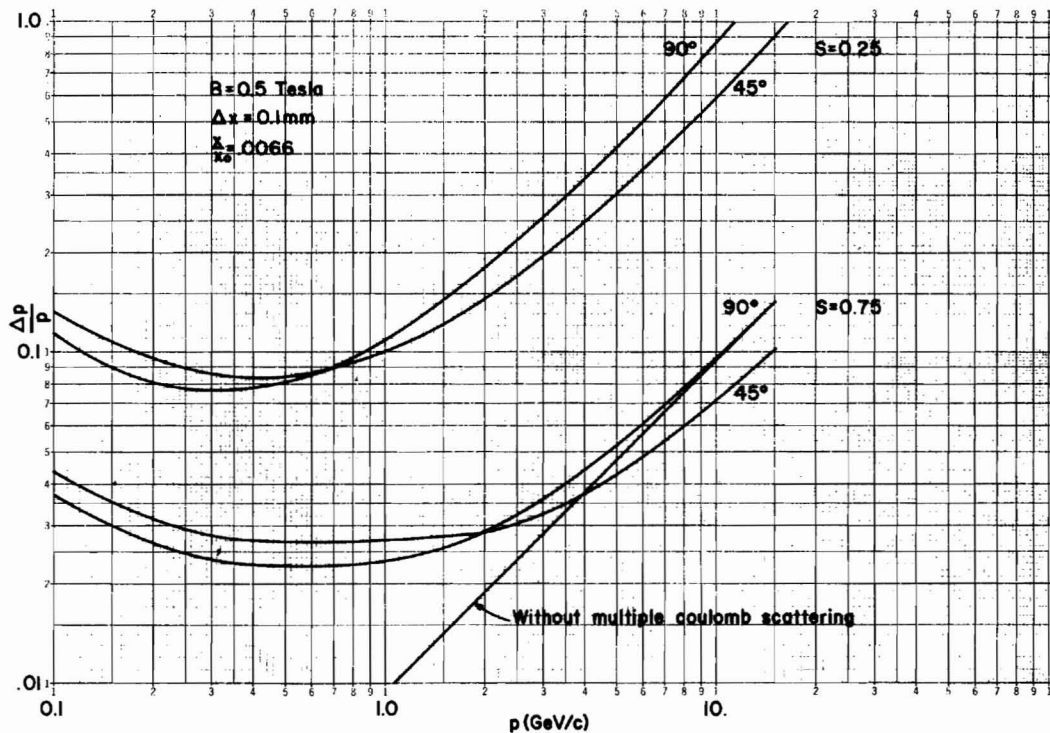


Fig. 4.

XBL 7410-1951

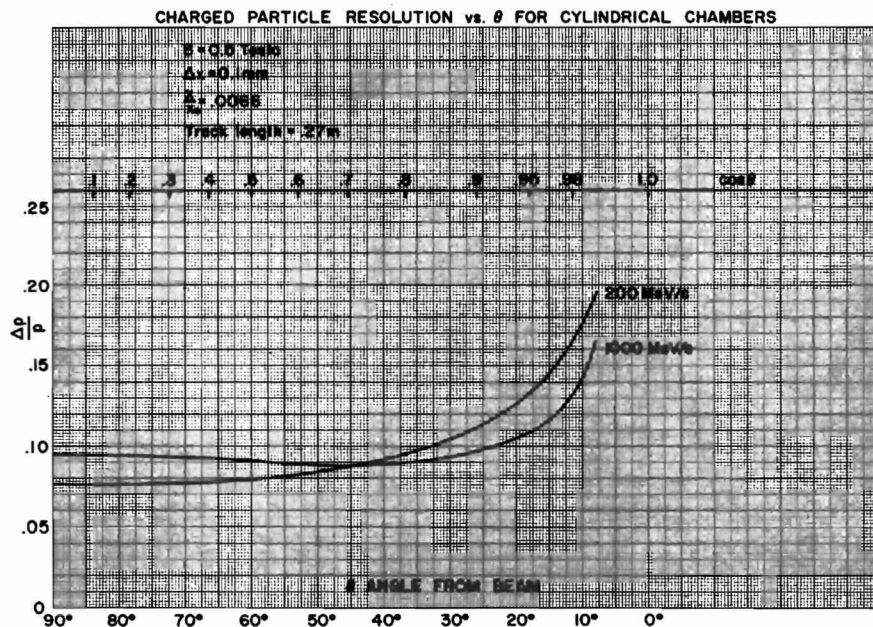


Fig. 5.

XBL 7410-1952

5. Particle Identification

This section deals with methods of distinguishing charged pions, kaons and protons.

Introduction

For many purposes at PEP, SPEAR and other accelerators it is important to distinguish the particle type as well as measuring its momentum. Here we will assume the momentum has been determined with complete precision and discuss the power of different techniques to identify particles. Among five major ways to identifying particles; time of flight, ionization loss, Cerenkov light, range, and decay characteristics, we will only discuss the first three. The last two have been considered briefly, but were not felt to be generally useful for the particle momenta considered. The three methods discussed are each techniques for measuring the particle velocity, hence with its momentum, finding its mass. Since these techniques can form independent measurements of β (or m), their use in combination could prove more powerful than any one type alone.

Time of Flight

The difference in time of flight between π 's and K's or p's is given by

$$\Delta t = \frac{d}{c} \left[\frac{1}{\beta_{K,p}} - \frac{1}{\beta_{\pi}} \right]$$

where d is the measurement distance

or

$$\Delta t = \frac{d}{cp} \left[\sqrt{p^2 + m_{K,p}^2} - \sqrt{p^2 + m_{\pi}^2} \right].$$

Figure 6 shows $\frac{\Delta t}{d}$ (ns/m) plotted against the momentum for π -K and π -p mass differences. In a highly tuned system one might hope to achieve $\pm .25$ ns resolution. Requiring a two standard deviation effect with this resolution

in a flight path of 0.5 meters one could separate π 's from K's up to about 550 MeV/c and π 's from p's up to about 1.0 GeV/c.

Ionization Loss

One can describe the ionization loss approximately by

$$\frac{dE}{dx} = \frac{DZ}{A\beta^2} \left[\ln \left(\frac{2m c^2 \beta^2 T_{\max}^I}{(1-\beta^2) I^2} \right) - 2\beta^2 - K \right]$$

(see p 66 of Apr 74 Particle Properties Booklet)

or for plastic scintillator

$$\frac{dE}{dx} \approx \frac{.08}{\beta^2} \left[20. + \ln \left(\frac{\beta^2}{1-\beta^2} \right) - 2\beta^2 \right] \text{ MeV} - \text{cm}^2/\text{g}.$$

Figure 7 shows the fractional difference between π -K and π -p ionization losses as a function of momentum. While the number of photons produced by ionization loss in scintillator is large, the Landau fluctuations limit the resolution of any measurement of ionization loss. It is probably difficult to achieve an energy loss resolution much better than $\pm .1$ due to these fluctuations. With a two standard deviation effect and a resolution of $\pm .2$ in Δ we could separate π 's from K's to 600 MeV/c and π 's from p's to about 1.1 GeV.

Cerenkov Light

The spectrum of Cerenkov light is given by

$$N(\lambda) = \frac{2\pi\alpha}{\lambda^2} \left(1 - \frac{1}{\beta^2 n^2} \right)$$

where n is the index of refraction.

By integrating this spectrum times the quantum efficiency of a phototube one can write

$$\# \text{photoelectrons/cm of pathlength} = N_0 \left(1 - \frac{1}{\beta^2 n^2} \right)$$

The integration for a bialkali PMT (RCA 8575) yields $N_0 = 210$.

Actual measurements of this parameter (Duteil et al 1968 CERN Rep. 68/14) give a more conservative value of $N_0 \approx 100$. For any actual system collection and transmission losses must be considered. Two general types of Cerenkov counters are considered: high index of refraction where pulse height analysis has some value, and low index of refraction where the device acts primarily as a threshold counter.

A. High Index

For indices in the range 1.3 - 1.7 a variety of transparent materials exist. With this high index, a large number of photons are produced and some pulse height analysis can be done. The fractional difference in photon yield can be written as

$$\Delta = \frac{C_{\pi} - C_{K,p}}{C_{\pi}}$$

or

$$\Delta = \frac{m_{k,p}^2 - m_{\pi}^2}{p^2 (n^2 - 1) - m_{\pi}^2}$$

This fractional difference is plotted versus momentum in Fig. 8 for $n = 1.3$, 1.5 and 1.7 for π -K and π -p differences. Note the maximum difference ($\Delta=1$) is at threshold. A well designed counter might have a sensitivity of about ± 0.15 for a few cm thickness. Recall lead glass can achieve $\pm .05$ or less for long Cerenkov path lengths.

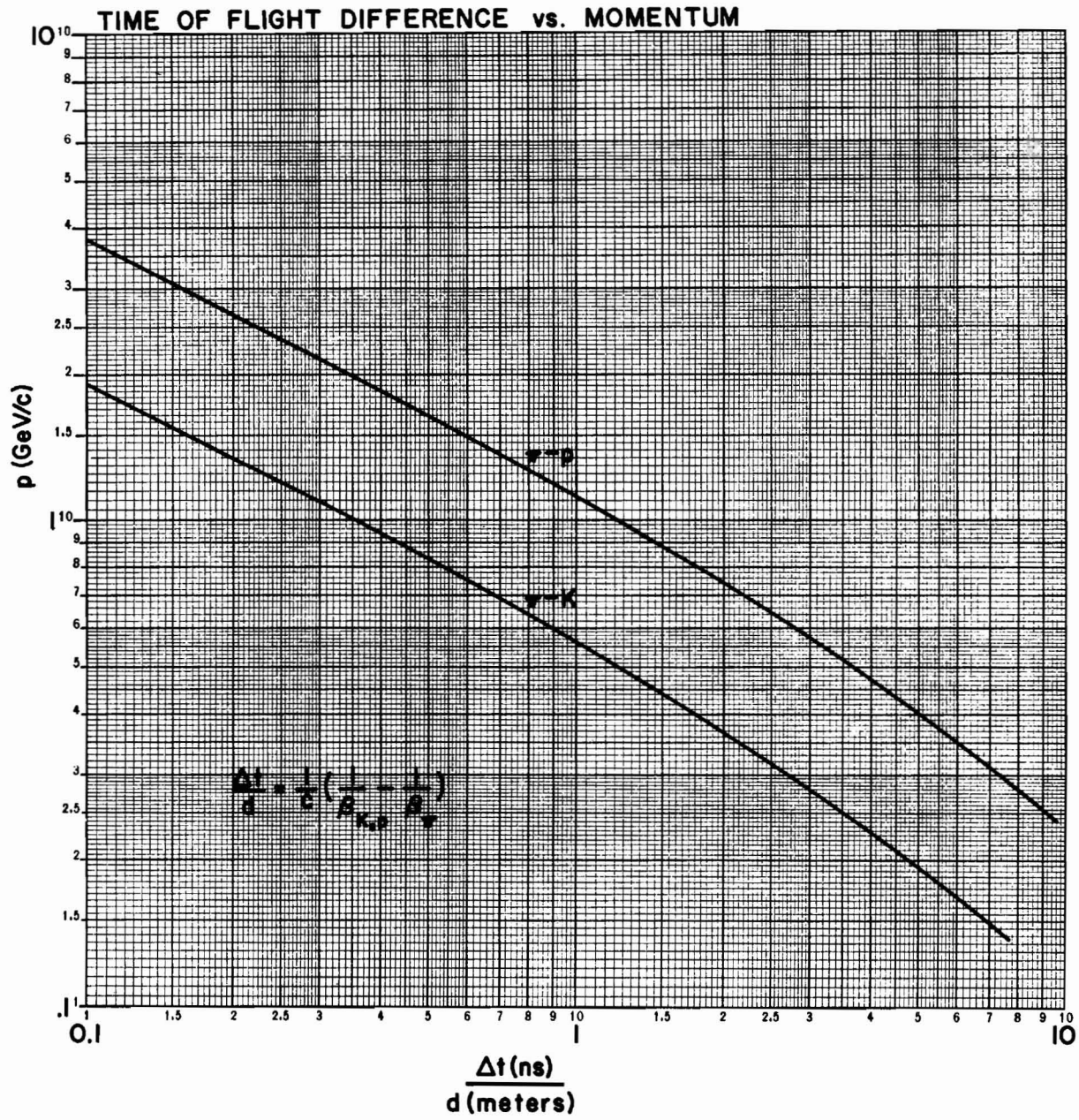
B. Low Index

Gases are the most likely materials in this range, although liquid hydrogen appears possible for some applications. For low indices the photon yield is low, so long path lengths are required and pulse height discrimination

is poor. For low index materials, a useful approximation is

$$N_e \approx N_o \left[2(n-1) - \left(\frac{m}{p} \right)^2 \right]$$

To facilitate the design of such detectors, the photoelectron yield using $N_o = 100$ (for 100% light collection onto a PMT) is plotted as a function of $n-1$ and momentum. Fig's 9, 10, and 11 show curves of constant photoelectrons for π 's K's and p's. Note the curve labeled 0 is just the threshold for Cerenkov light. For a real counter the light collection efficiency must be estimated to find the number of photoelectrons seen and thus to estimate the counter efficiency and resolving power. Fig. 12 indicates the refractive index of some useful gases as a function of pressure at typical room temperatures. (Hayes et al, ANL-6916, Handbook of Chem. & Phys.)



XBL 7410-1966

Fig. 6.

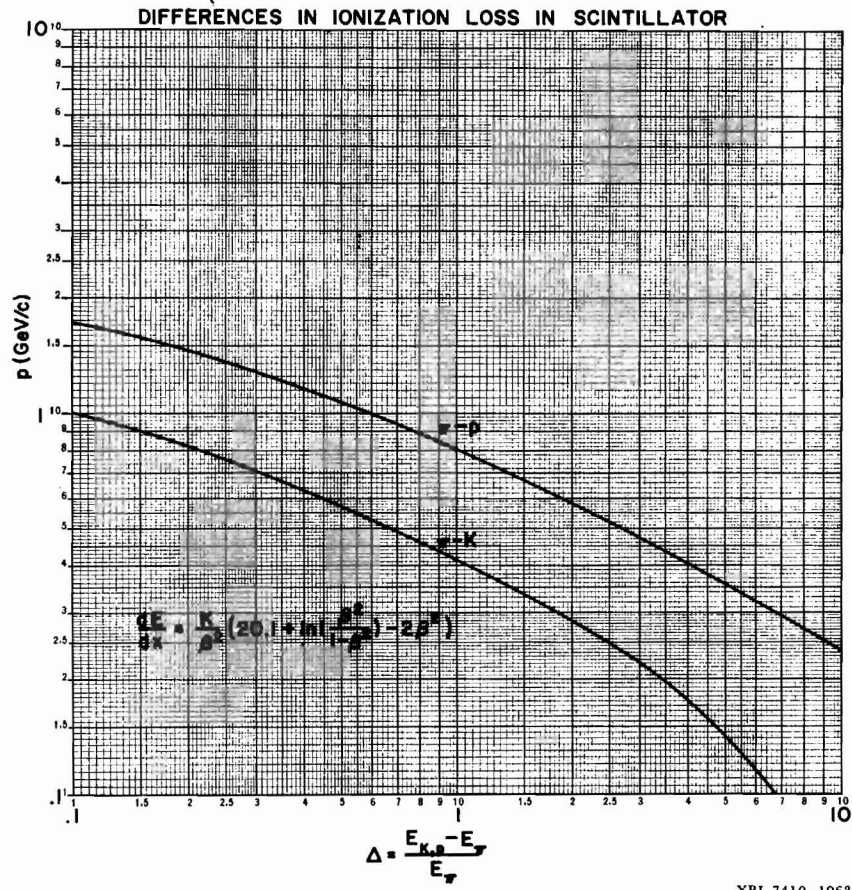


Fig. 7.

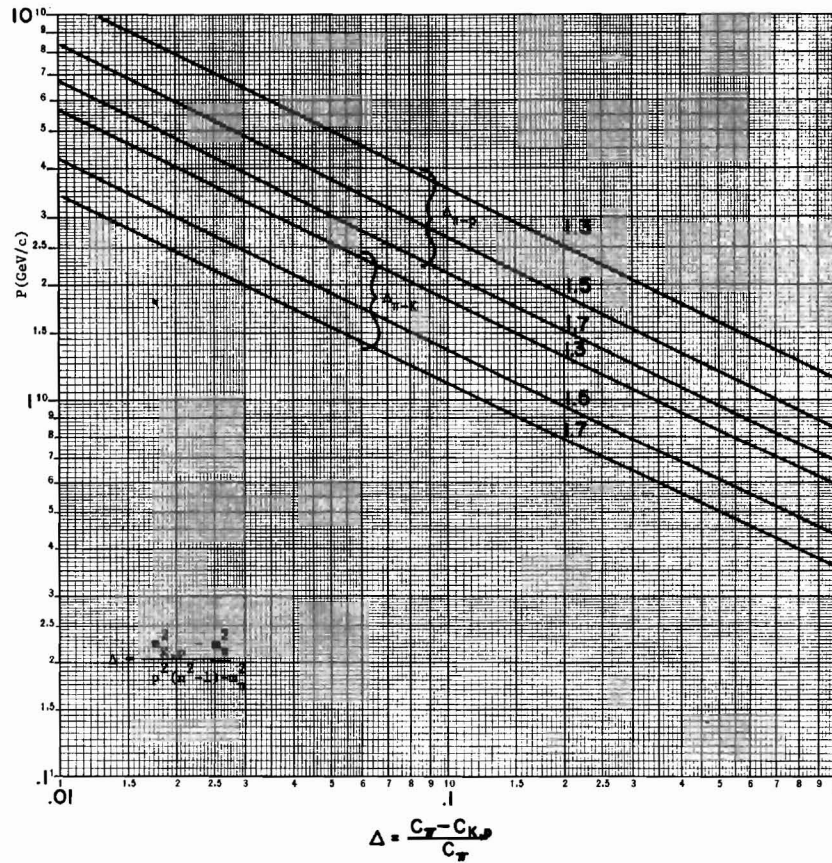
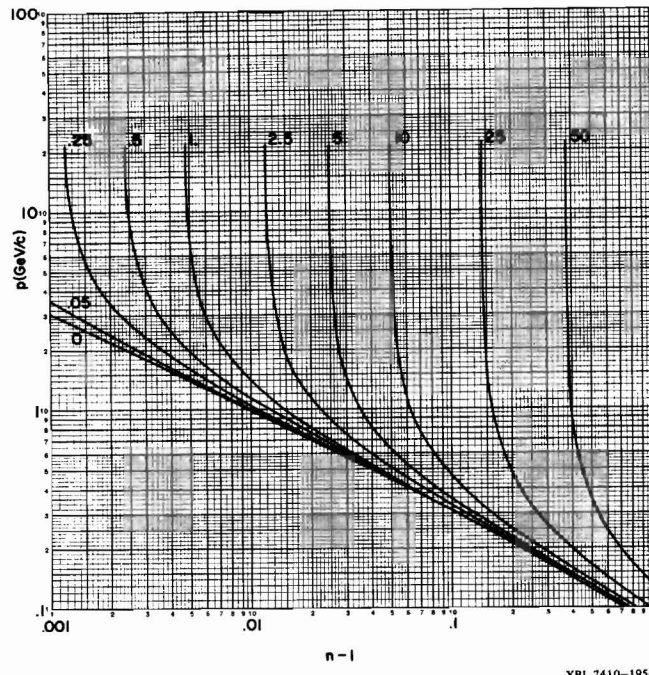
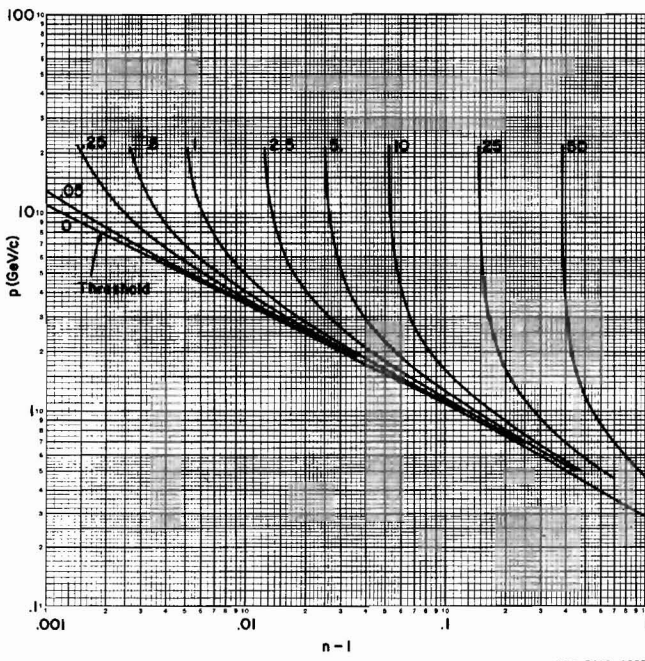


Fig. 8.



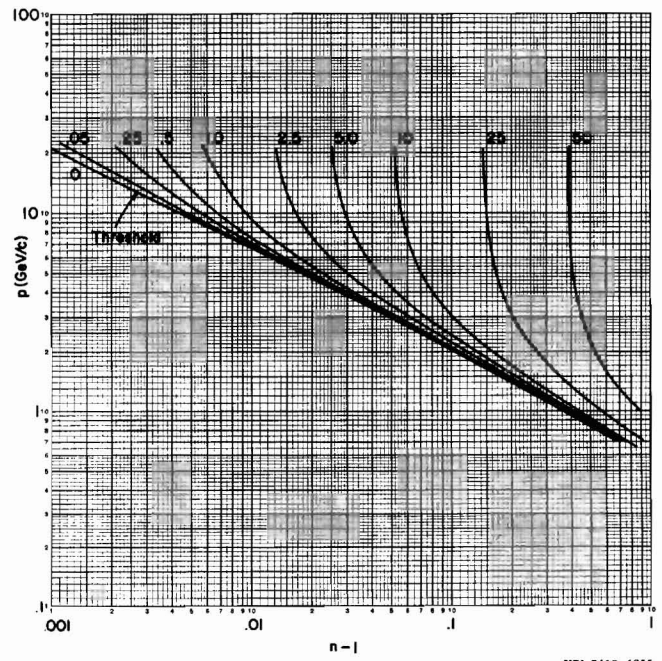
XBL 7410-1954

Fig. 9.



XBL 7410-1953

Fig. 10.



XBL 7410-1955

Fig. 11.

Results

The resolving powers of the various identification schemes are shown in Fig. 13. The solid lines indicate reasonable possibilities, (assuming a carefully calibrated detector) the dashed portions more speculative regions.

TOF: 2σ values of $\frac{\Delta t}{d} < 1$ ns/m are probably difficult to achieve even with large systems because of the large dimensions of the scintillator needed in 4π type geometry.

Ionization: 2σ values of Δ of .2 are probably achievable by careful calibration

Cerenkov: 2σ values of Δ of .3 appear attainable
n=1.5

Cerenkov: This requires approximately 27 atmospheres pressure and with
n=1.03
10 cm path length yields about 60 photoelectrons x (geometrical efficiency). If some pulse height discrimination is possible the momentum region might be extended into the dashed regions

Cerenkov: This requires about 17 atmospheres pressure and with 20 cm
n=1.015
path length yields about 60 photoelectrons x (geometrical efficiency). If some pulse height discrimination is possible the momentum region might be extended into the dashed regions.

In conclusion, it appears possible to achieve good particle separation up to 2 to 4 GeV for K's and p's respectively using carefully designed and calibrated apparatus. These detectors have minimal bulk and could possibly be included in a compact neutral plus charged detector.

6. Resolution of a Neutral Particle Detector

This section limits itself to the discussion of γ ray detection and its implications.

Motivation

In reactions where many particles occur in the final state, and some of them are π^0 , η 's or other particles decaying into γ rays, proper pairing of the γ rays is necessary in order to study in any detail the dynamics of the decaying particles. A powerful technique for identifying the correct pairing of γ rays is to calculate the candidate pairs invariant mass and compare this against the masses of known particles (π^0 , η , etc). Presumably the achieved mass resolution is a good measure of the quality of a neutral particle detector. Using this mass resolution as a figure of merit, we discuss the implications of various γ detection systems.

Kinematics

For simplicity only the decay of particles into 2 γ rays is analyzed here. Defining the decaying particle and final γ rays as particles 0, 1, and 2 respectively, we can write the kinematic equation

$$m_o^2 = 2E_1E_2(1-\cos\theta_{\gamma\gamma})$$

Where $\theta_{\gamma\gamma}$ is the angle between the 2 γ rays

Using this one can easily obtain

$$\frac{(\delta m_o)^2}{m_o^2} = \frac{2\delta m_o}{m_o} = \left[\left(\frac{\sin\theta_{\gamma\gamma}}{1-\cos\theta_{\gamma\gamma}} \right)^2 \delta^2\theta_{\gamma\gamma} + \left(\frac{\delta E_1}{E_1} \right)^2 + \left(\frac{\delta E_2}{E_2} \right)^2 \right]^{1/2}$$

rewriting $\Theta_{\gamma\gamma}$ in terms of E_1 and E_2 one obtains

$$\frac{\delta m}{m} = \frac{1}{2} \left[\left(\frac{4E_1 E_2}{m_0^2} - 1 \right) \delta \Theta_{\gamma\gamma} + \left(\frac{\delta E_1}{E_1} \right)^2 + \left(\frac{\delta E_2}{E_2} \right)^2 \right]^{1/2}$$

For a given E_0 , a range of values of E_1 or E_2 are possible, subject to $E_0 = E_1 + E_2$. For a spinless particle 0, the γ energies are distributed uniformly in α with

$$E_1 = \alpha E_0$$

$$E_2 = (1-\alpha)E_0$$

$$\text{with } \alpha_{\min} = \frac{E_0 - P_0}{2E_0}, \quad \alpha_{\max} = \frac{E_0 + P_0}{2E_0}.$$

Using this, it is straight forward to average over possible α 's (with a computer), and in fact the mass resolution is almost independent of α . Now we must make some models of the errors and study the consequences.

Errors

The assumed energy resolution was put in the form

$$\frac{\delta E}{E} = \beta E^{-n} \quad E \text{ in GeV}$$

with 3 cases considered

$$\left. \begin{array}{l} \beta = 0.05 \\ n = 0.5 \end{array} \right\} \text{Lead Glass}$$

$$\left. \begin{array}{l} \beta = 0.01 \\ n = 0.25 \end{array} \right\} \text{NaI}$$

$$\beta = 0 \quad (\Delta E = 0)$$

The spatial resolution was estimated for various cases:

- (1) 2 sets of $2x_0$ active converters followed by proportional chambers to measure the shower position. A Monte Carlo shower program gave position resolution for this geometry consistent with the formula

$$\Delta x = 0.18 E_{\gamma}^{-0.65} \quad E_{\gamma} \text{ in GeV, } \Delta x \text{ in centimeters.}$$

- (2) The same as (1) above, but the spatial resolution was limited to 0.5 cm (by the proportional chambers).

- (3) Constant spatial resolution as one might find in a simple hodoscope of Lead Glass blocks with

$$\Delta x = 3.0 \text{ cm.}$$

- (4) $\Delta x = 0.0$

The error in $\theta_{\gamma\gamma}$ is

$$\delta\theta_{\gamma\gamma} = \left[(\Delta x_1)^2 + (\Delta x_2)^2 \right]^{1/2} / R$$

where Δx is the one-dimensional position uncertainty and R is the radius of measurement.

- (5) Constant angular error for each γ $\Delta\theta_{\gamma} = c$

$$\text{so } \Delta\theta_{\gamma\gamma} = \sqrt{2} \Delta\theta_{\gamma}$$

Results

Representative combinations of the above error models were used to make mass resolution calculations as a function of π^0 momentum (averaging over allowed α). Fig. 14 shows the mass resolution for Pb-Glass and NaI with perfect spatial resolution. Also shown are curves of perfect energy resolution and constant angular resolution (for each γ). From these curves the resolution of a real system can be constructed by adding the appropriate pair of curves in quadrature. In Fig. 15, mass resolutions are calculated for a real geometry ($R=60$ cm) and various assumptions.

Lead Glass

- (a) $\Delta\theta = 0$
- (b) $\Delta\theta$ defined by (1)
- (c) $\Delta\theta$ defined by (2)
- (d) $\Delta\theta$ defined by (3)

NAI

- (a) $\Delta\theta = 0$
- (b) $\Delta\theta$ defined by (1)

$\Delta E = 0$, $\Delta\theta$ defined by (1)

One should perhaps keep in mind that for high momentum π^0 's the opening angle is sufficiently small that pairing confusion is reduced consequently the reduced high momentum mass resolution achieved in some cases considered is not as damaging as one might first imagine.

π^0 opening angle probability distributions are shown in Fig. 16

$$\theta_{\gamma\gamma}^{\min} = 2 \cos^{-1} \beta_{\pi^0}$$

$$P(\theta_{\gamma\gamma} \leq u) = \sqrt{\frac{\sin^2 u/2 - 1/\gamma^2}{\beta \sin u/2}}$$

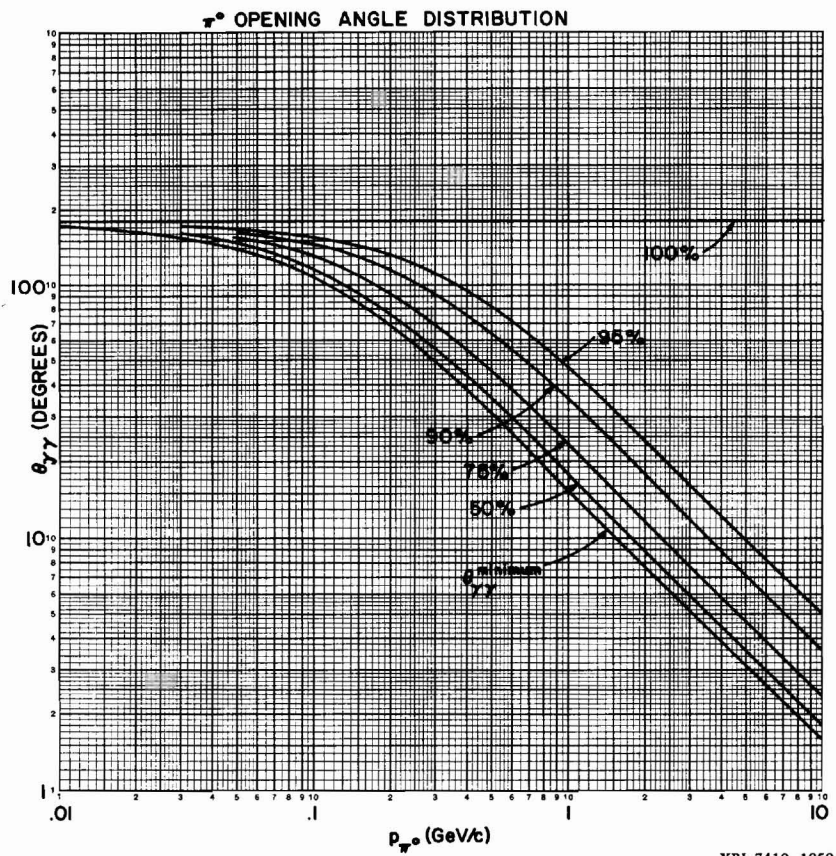


Fig. 16.

7. Cost of the Neutrals Detector

The high cost of lead-glass and NaI make the neutrals detector a strong constraint on any design. We perform a simple exercise here and calculate the volume of lead glass needed to cover a cylinder with a layer 12 radiation lengths thick. The volume of course is only the beginning of a real detector. The number of pieces, their shapes, and the surface treatment have significant effects on the cost. The sketch below shows the geometry of the lead glass "blanket." The blanket is padded so all gammas see the same number of radiation lengths.

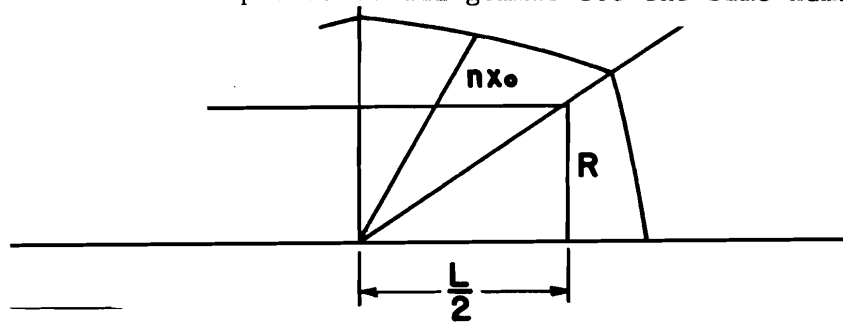


Figure 17 shows the integrated volume of this blanket versus cylinder radius for various aspect ratios (L/R). To a good approximation the volume is proportional to the number of radiation lengths and the solid angle covered. Since lead glass costs about $\$100,000 / \text{m}^3$ a cylinder 0.5 m in radius and 2.0 m long would cost $\$360,000$ to cover except for the fact that many pieces with odd angles would be required to achieve this geometry. This would increase the cost by a factor of 1.5 or more. Using rectangular blocks would require more volume but would save on cutting and polishing costs.

Hybrid Gamma detectors.

Is it possible to use two detection techniques to improve the energy resolution of low energy gammas? For example, can we use NaI (good but expensive) to get good energy resolution on low energy gammas followed by lead-glass (poorer resolution but not as expensive) to get the higher energy gammas?

For this to be feasible we cannot have too large a fraction of the low energy showers extend into the lead glass. Let E be the energy of the gamma (GeV), $R_1(E)$ and $R_2(E)$ be the resolutions of the detectors ($\Delta E/E$), t the thickness of detector #1, and $f(t,E)$ be the fraction of the shower that escapes the first detector and is measured in #2. The final resolution will be

$$R = \frac{\delta E}{E} = \left[(1-f)^2 R_1^2 ((1-f)E) + f^2 R_2^2 (fE) \right]^{1/2}$$

If we take the case of NaI and lead-glass,

$$R_1 = .009/E^{.25}, \quad R_2 = .05/E^{.5}$$

Figure 18 shows R as a function of f for various energy gammas. When $f=1$ on the right hand side the resolution is that of all lead-glass; when $f=0$ on the left the resolution is for pure NaI. A shower monte carlo program has been used to calculate the fraction of a shower escaping 2, 4, 6, and 8 radiation lengths of NaI and these give rise to the vertical curves. For a 50 MeV gamma to the resolution goes from 22% for pure lead glass to 10% with the first 6 radiation lengths being replaced by NaI. For a small detector this might be feasible. For large solid angle detectors at SPEAR and PEP this becomes fairly expensive. Since the cost of NaI is about 5 times the cost of lead-glass, using 6 radiation lengths of NaI would triple the cost of a 12 radiation length detector.

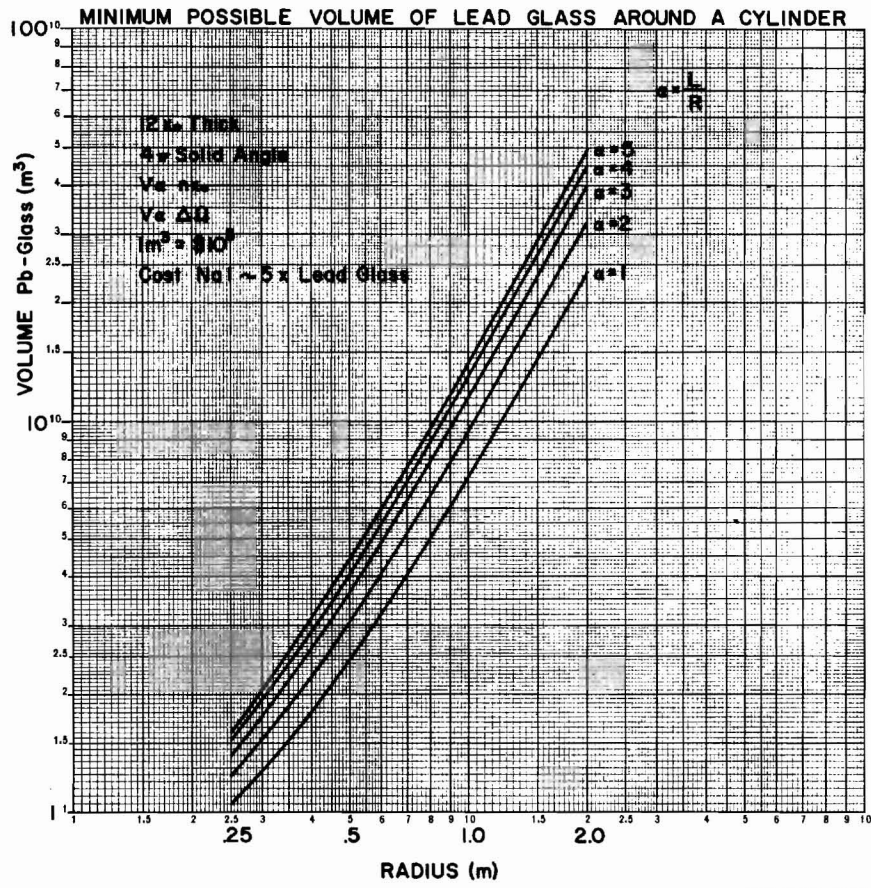


Fig. 17.

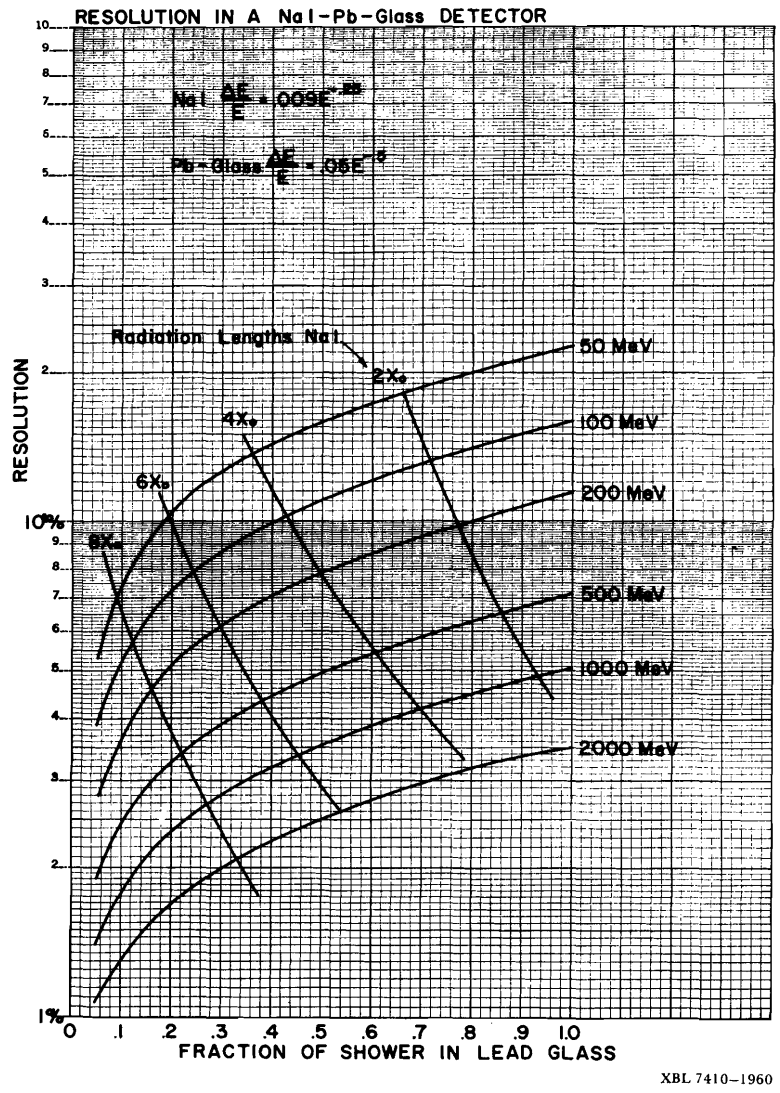


Fig. 18.